Trans Indian Inst Met (2018) 71(11):2855–2859
https://doi.org/10.1007/s12666-018-1413-x

TECHNICAL PAPER

Effect of Multiple Reflow Cycles on the Shear Strength of Nano-Al_2O_3 Particles Reinforced Sn3.6Ag Lead-Free Solder Alloy

Sanjay Tikale[1] · K. Narayan Prabhu[1]

Received: 31 July 2018 / Accepted: 6 September 2018 / Published online: 19 September 2018

Abstract The effect of nano-Al_2O_3 particles reinforcement on shear strength of Sn3.6Ag solder joint exposed to multiple reflows was studied. The nano-composites of Sn3.6Ag solder were developed by mechanical dispersion of nanoparticles in the solder alloy. The melting, mechanical and microstructural properties of Sn3.6Ag composite solders with varying weight fractions of nano-Al_2O_3 particles were evaluated by subjecting them to multiple reflow cycles. The results showed an improvement in the wettability of the solder with inclusion of nano-Al_2O_3 particles. The composite Sn3.6Ag solders with 0.01–0.05 wt% nanoparticles reinforcement showed an improvement in the shear strength and ductility of the solder joint compared to monolithic solder alloy under multiple reflow cycles. Samples doped with 0.05 wt% nanoparticles and reflowed for two reflow cycles displayed an appreciable suppression in interfacial intermetallic compound's growth and improvement in the solder joint shear strength. The addition above 0.1 wt% in solder showed a decrease in the beneficial effects of nano-Al_2O_3 particles reinforcement.

Keywords Multiple reflow cycles · Nano-Al_2O_3 particles · Nano-composite · IMC growth · Shear strength

✉ K. Narayan Prabhu
prabhukn_2002@yahoo.co.in

Sanjay Tikale
Sanjaytikale@gmail.com

[1] Department of Metallurgical and Materials Engineering, National Institute of Technology Karnataka, Surathkal 575 025, India

1 Introduction

An electronic assembly frequently experiences various mechanical and thermal stresses during its production, repair, transport, storage and operation. Therefore, an optimum performance of the solder is vital to the reliability of a solder joint, which is essential for the high functionality of electronic products [1, 2]. The demand for higher functionality in electronic products and miniaturization of interconnects has motivated the research and development of high performing lead-free solders [3]. The binary and ternary lead-free solder alloys based on Sn–Cu, Sn–Ag and Sn–Ag–Cu alloy systems are promising options for replacement of conventional Sn–Pb solders [4]. The addition of appropriate nanoparticles into the solder alloy has proved to be an effective way of improving the mechanical performance of the solder. The non-reacting nanoparticles act as a second-phase material in the solder alloy matrix which provides extra nucleation sites during solidification which in turn refines the solder grain structure and improves the solder joint reliability. Research in this area suggests that the ceramic nanoparticles reinforcement in the solder alloy effectively improves the solder properties [5, 6]. Dispersed nanoparticles and intermetallic phases block the dislocation movements in the matrix which improves the solder shear strength during failure. The adsorption of nanoparticles on IMC surface limits the diffusion of related element and suppresses the IMC growth at the interface [7]. The present study investigates the effect of nono-Al_2O_3 particles reinforcement in different weight fractions on the joint reliability of Sn3.6Ag solder alloy under various reflow cycles.

2 Experimental Methodology

2.1 Assessment of Melting Behavior and Wettability of Composite Solder

Commercial 96.4Sn–3.6Ag (in wt%) solder alloy paste added with rosin mildly activated flux was used as the base alloy. Nano-Al_2O_3 particles (average particle size of 20–30 nm) were treated with polyvinylpyrrolidone (PVP-10) surfactant in dimethylacetamide (DMAc) solution before reinforcement. Four composite solder systems were prepared by mechanical dispersion of the treated nano-Al_2O_3 particles in 0.01, 0.05, 0.1 and 0.5 wt%, respectively, into the solder using stirrer. These composite solder compositions are labeled hereafter as, Sn3.6Ag–xAl_2O_3 where x represents weight percentage addition of nanoparticles. Differential scanning calorimetry (DSC) was used to assess the melting behavior of different Sn3.6Ag nano-composites. The wettability of composite Sn3.6Ag solder alloys was assessed with respect to the spreading area of reflowed samples. The composite solder paste of 0.1 gm weight was dispensed on the copper substrate and reflowed using reflow oven. Samples after reflow cycles were analyzed by measuring their spreading area using stereomicroscope (STEMI 2000C) and image analyzer software.

2.2 Joint Shear Test

Joint shear strength and ductility of the solder joint were examined by using the pull test on soldered single-lap-shear joint samples. Figure 1 shows the schematic of the solder joint sample. A rectangular layer (0.1 gm in weight) of solder paste was placed between two copper plate substrates and reflowed using programmable reflow oven. The thermal profile used for reflow process is represented in Fig. 2. The effect of nanoparticles reinforcement on joint strength and interfacial microstructure under multiple reflows was investigated using samples reflowed for 1, 2, 4 and 6 cycles, respectively. The tensile pull test was carried out to assess the joint shear strength using the strain rate of 1×10^{-2} s^{-1} on the tensile tester (Instron 5967, 30 kN). The average joint shear strength was determined from the obtained stress–strain curves for different Sn3.6Ag solder compositions.

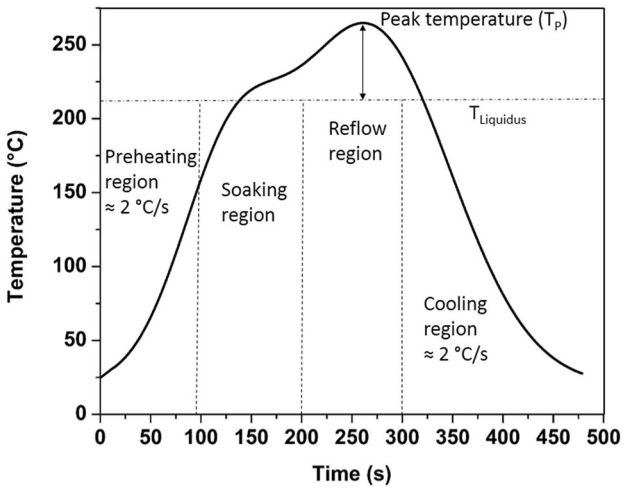

Fig. 2 Temperature reflow profile for solder joint preparation

2.3 Microstructure Study

The microstructural evolution and intermetallic layer growth with nano-Al_2O_3 particles reinforcement under multiple reflow cycles at the joint interface were studied using scanning electron microscopy (SEM). The elemental compositions of different phases were analyzed with the help of energy-dispersive spectroscopy (EDS) and X-ray diffraction spectroscopy (XRD). Reflowed samples were polished with standard polishing technique. Polished surfaces were etched with an etchant [92% CH_3OH + 5% HNO_3 + 3% HCL] for 1–2 s and observed under SEM. The interfacial IMC thickness was measured using image analyzer (Axio Vision SE64 Rel. 4.9) software.

3 Results and Discussion

3.1 Melting Properties and Wettability of Solder

The change in melting temperature range and pasty range of Sn3.6Ag solder alloy with various compositions of nano-Al_2O_3 particles obtained from DSC analysis are presented in Table 1. The addition of 0.01–0.1 wt% nanoparticles shows a slight decrease in the melting temperature range as well as pasty range of Sn3.6Ag solder alloy. The dispersed surface-active nano-Al_2O_3 particles in

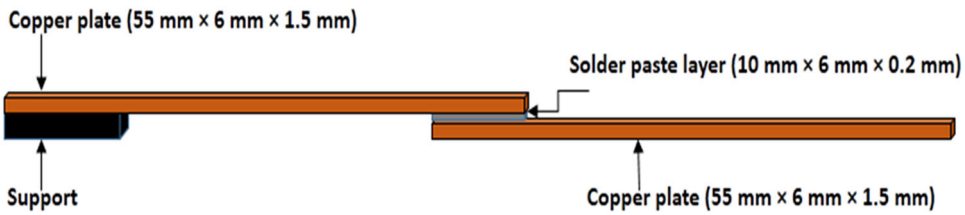

Fig. 1 Representation of the single-lap-shear solder joint

Table 1 Peak melting temperature, pasty range and melting temperature range of Sn3.6Ag solder with various nano-Al_2O_3 particles compositions

Solder composition	T_{Onset}, heating (°C) **A**	T_{Peak}, heating (°C) **B**	T_{Endset}, heating (°C) **C**	Pasty range (°C) **(C–A)**	Melting temperature range (°C) **(B–A)**
Sn3.6Ag	221.84	225.77	228.17	6.33	3.93
Sn3.6Ag–0.01Al_2O_3	221.44	224.99	226.98	5.54	3.55
Sn3.6Ag–0.05Al_2O_3	220.58	224.05	226.01	5.43	3.47
Sn3.6Ag–0.1Al_2O_3	220.6	224.21	226.52	5.92	3.61
Sn3.6Ag–0.5Al_2O_3	220.71	224.66	227.19	6.48	3.95

molten solder add excess surface free energy and increases the instability in the molten solder. Nanoparticles also provide the additional sites for heterogeneous nucleation which reduce the onset temperature of solder and promote solidification. The decrease in pasty range of the solder alloy improves the reliability of the joint. Particularly, 0.05 wt% nano-Al_2O_3 particle addition shows an appreciable improvement in the solder melting characteristics. However, the addition of nano-alumina particles above 0.1 wt% increases the agglomeration of nanoparticles which reduces the amount of dispersed active material in the molten solder leading to decrease in the beneficial effects of the nanoparticles addition.

Figure 3 shows the plot for spreading area versus different wt% of nano-Al_2O_3 particles addition for Sn3.6Ag solder alloy. The 0.01–0.5 wt% nanoparticles addition shows the consistent improvement in spreading area of the Sn3.6Ag solder alloy. The extent of increase in spreading area directly implies an increase in the wettability. The presence of surface-active nanoparticles significantly alters the grain boundary/interfacial energies which in turn reduces the surface tension of the solder melt and also decreases the solder/substrate interfacial tension. This leads to the enhancement in the spreading of liquid solder and thus improves the wettability of the solder alloy.

3.2 Solder Joint Microstructure and Intermetallic Compound Growth

The solidified Sn3.6Ag/Cu joint microstructure mainly consists of dispersed spheroidal and plate shaped Ag_3Sn IMC in β-Sn matrix and Cu_6Sn_5 as well as Cu_3Sn IMC layers at the solder/substrate interface. The size and morphology of Cu_6Sn_5 and Cu_3Sn IMC changes with repeated exposure to the reflow cycles. Figure 4 represents the average Cu_6Sn_5 and Cu_3Sn IMC layer thickness under different reflow cycles for different composite Sn3.6Ag solders. Figure 5 shows the SEM micrographs of reflowed samples for composite Sn3.6Ag solder joint interface reflowed for various reflow cycles. The Cu_6Sn_5 IMC morphology for unreinforced Sn3.6Ag solder is found to be scallop shaped. The IMC grows as elongated

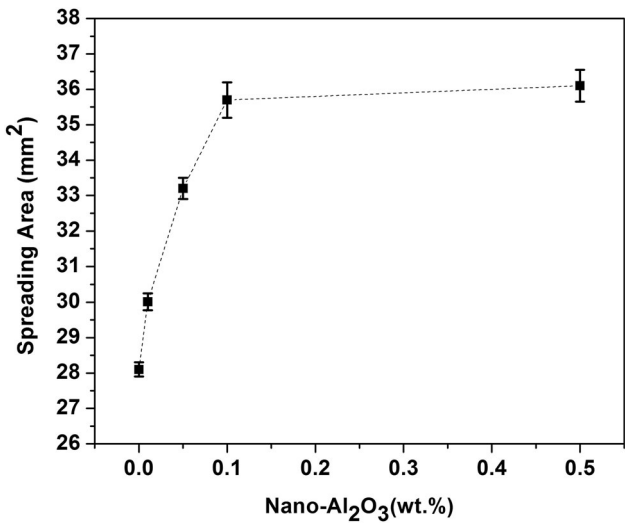

Fig. 3 Spreading area versus weight fraction addition of nano-Al_2O_3 particles

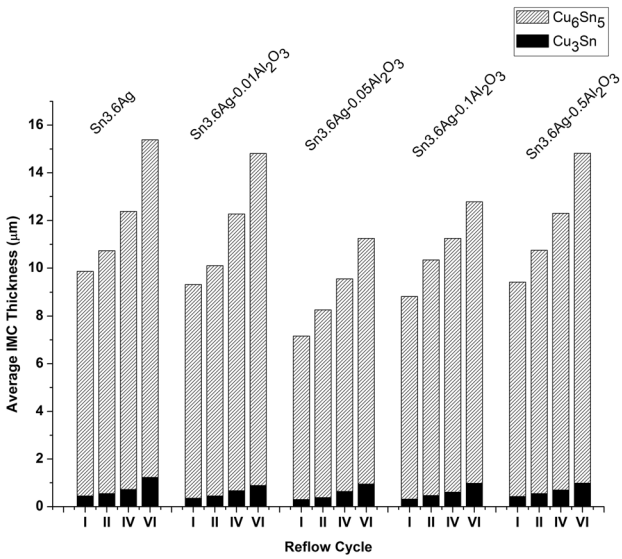

Fig. 4 Average IMC thickness under multiple reflow cycles

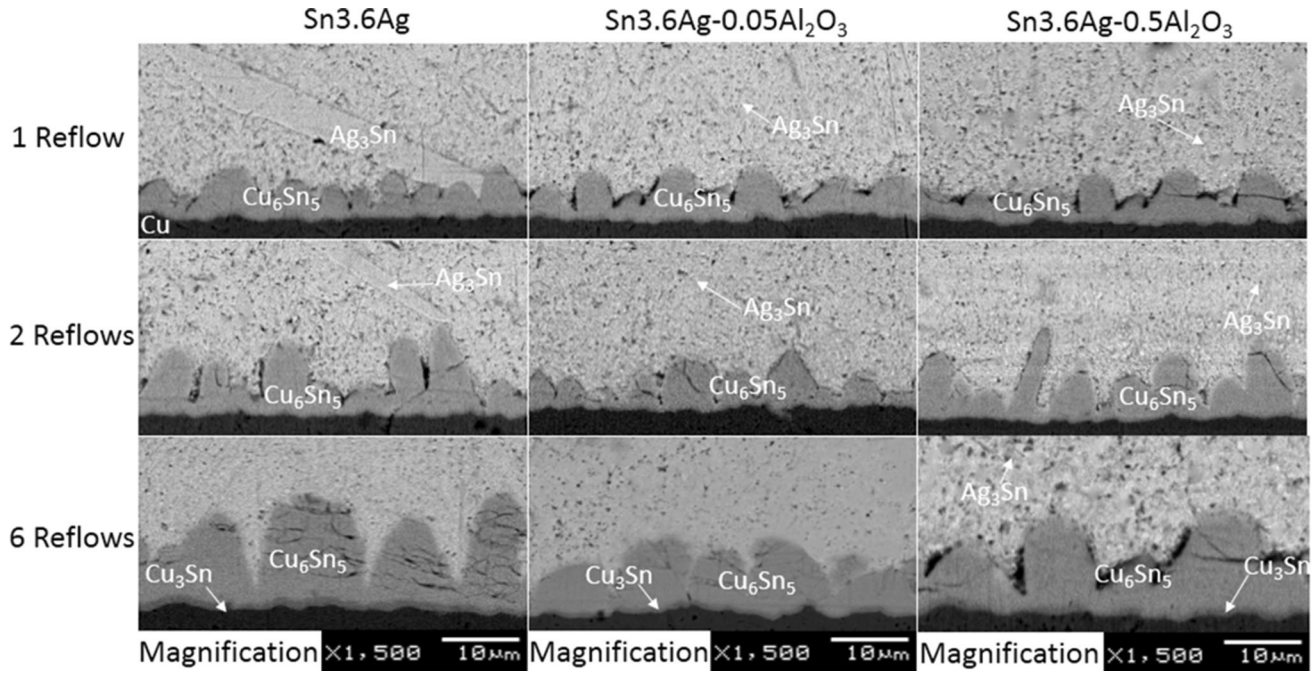

Fig. 5 SEM images of solder/Cu joint interface under different reflows for Sn3.6Ag composite solder alloys

and coarser scalloped form with the increase in reflows. The thickness of Cu_3Sn IMC layer increases with multiple reflow cycles.

The nano-Al_2O_3 particles reinforcement in Sn3.6Ag solder retard the Cu_6Sn_5 IMC layer growth and refine the plate-shaped Ag_3Sn IMC into fine-spheroidal form in the matrix under repeated exposure to reflow cycles. The uniform distribution of fine-spheroidal Ag_3Sn IMC along with nano-Al_2O_3 particles acts like second-phase particles which enhances the solder strength under applied stress. The hindrance of IMC layer growth can be attributed to the surface-active nanoparticles adsorption on IMC surface. The nanoparticles adsorption on IMC reduces its surface energy which in turn decreases the growth rate of IMC formation leading to the suppression of Cu_6Sn_5 IMC growth and refinement of Ag_3Sn IMC in the solder bulk. In this study, the most effective Cu_6Sn_5 IMC growth suppression under repeated reflow cycles can be obtained with 0.05 wt% nano-Al_2O_3 particles addition compared to other compositions. The effective adsorption of nanoparticles on Cu_6Sn_5 IMC reduces the diffusion of Sn from bulk solder to the IMC and also blocks the dissolution of Cu from Cu_6Sn_5 IMC into the bulk solder which results in suppression of the growth of IMC layer under repeated reflows. The ineffectiveness of high weight fraction (0.5 wt%) nano-Al_2O_3 particles addition in retardation of IMC growth can be attributed to the decrease in effective adsorption of nanoparticles on IMC due to agglomeration associated with excessive addition.

3.3 Solder Shear Strength

The joint shear strengths for different Sn3.6Ag–Al_2O_3 alloy compositions under multiple reflows are shown in the bar chart (Fig. 6). The addition of nanoparticles in 0.01–0.05 weight fractions enhances the joint strength and ductility of the joint compared to monolithic Sn3.6Ag as well as other compositions of solder under repeated reflow cycles. The shear strength of Sn3.6Ag solder alloy is observed to be increasing with second reflow cycle irrespective of the solder composition and decreases with higher reflows. The Sn3.6Ag–0.05Al_2O_3 composition

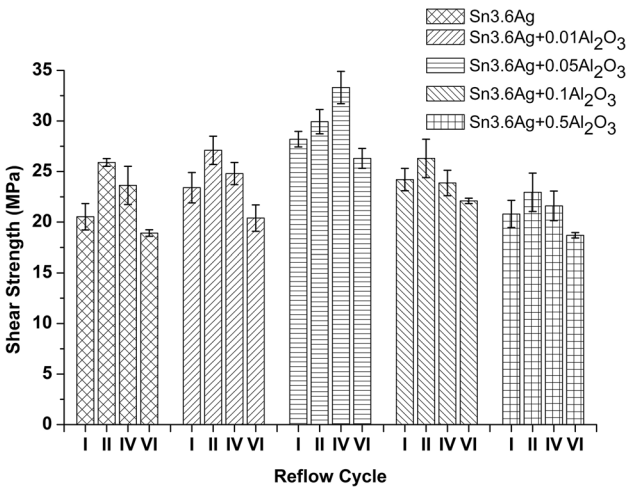

Fig. 6 Shear strength of Sn3.6Ag–Al_2O_3 alloy compositions for various reflow cycles

shows consistent increase in the joint strength and ductility up to 4 reflows among all compositions studied. The increase in joint shear strength can be attributed to the formation of continuous, thin and even Cu_6Sn_5 IMC at the interface along with the uniform scattering of finer-spheroidal Ag_3Sn IMC and nano-Al_2O_3 particles in bulk microstructure. The refinement of plate-shaped Ag_3Sn IMC into spheroidal form in bulk microstructure and coarsening of Sn grains with multiple reflows contribute to the improvement in joint ductility. On the other hand, high content (> 0.1 wt%) addition of nanoparticles reverses the beneficial effects of nanoparticles addition. The coarser and elongated Cu_6Sn_5 IMC and thick Cu_3Sn IMC layer at the interface often possesses micro-cracks. The thick and brittle IMC layer with micro-cracks significantly weaken the solder joint which considerably reduces the joint shear strength and ductility.

4 Conclusion

The nano-Al_2O_3 particles reinforcement slightly decreased the melting temperature range and pasty range of the Sn3.6Ag solder. The nano-composite solders exhibited enhanced solder wettability as compared to monolithic solder alloy. Irrespective of the solder composition, the joint strength of Sn3.6Ag solder alloy improved with second reflow cycle and gradually decreased with increase in reflows. The addition of 0.05 wt% nano-Al_2O_3 particles resulted in most effective retardation of the IMC growth, improved shear strength and ductility of the solder joint under multiple reflows. The nano-Al_2O_3 particles addition above 0.1 wt% nullifed all the advantageous effects of nanoparticles addition.

References

1. Yoon J W, Kim S W, Koo J M, Kim D G, and Jung S B, *J Electron Mater* **33** (2004) 1190.
2. Satyanarayan, Prabhu K, *Adv Colloid Interface Sci* **166** (2011) 87.
3. Abdelhadi O M, and Ladani L, *J Electron Packag* **135** (2013) 21004.
4. Tan A T, Tan A W, and Farazila Y, *Sci Technol Adv Mater* **16** (2015) 1.
5. Yakymovych A, Plevachuk Y, Svec Sr. P, Svec P, Janickovic D, Sebo P, Beronska N, Roshanghias A, and Ipser H, *J Electron Mater* **45** (2016) 6143.
6. Gain A K, Chan Y C, and Yung W K C, *Microelectron Reliab* **51** (2011) 2306.
7. Lee J S, Chu K M, Patzelt R, Manessis D, Ostmann A, and Jeon D Y, *Microelectron Eng* **85** (2008) 1577.